The Solvent–Gelator Interaction as the Origin of Different Diffusivity Behavior of Diols in Gels Formed With Sugar-Based Low-Molecular-Mass Gelator.

ARTICLE *in* THE JOURNAL OF PHYSICAL CHEMISTRY B · MARCH 2014

Impact Factor: 3.3 · DOI: 10.1021/jp412511e · Source: PubMed

THE JOURNAL OF PHYSICAL CHEMISTRY B

Article

pubs.acs.org/JPCB

The Solvent–Gelator Interaction as the Origin of Different Diffusivity Behavior of Diols in Gels Formed with Sugar-Based Low-Molecular-Mass Gelator

Joanna Kowalczuk,[†] Michał Bielejewski,[†] Andrzej Łapiński,[†] Roman Luboradzki,[‡] and Jadwiga Tritt-Goc*[,†]

[†]Institute of Molecular Physics, Polish Academy of Sciences, ul. M. Smoluchowskiego 17, 60-179 Poznań, Poland

[‡]Institute of Physical Chemistry, Polish Academy of Sciences, ul. Kasprzaka 44/52, 01-224 Warsaw, Poland

Supporting Information

ABSTRACT: Organogels are soft materials consisting of low-molecular-mass gelators (LMOGs) self-assembled through noncovalent interactions into 3D structures, in which free spaces are filled by organic solvents. 4,6,4′,6′-*O*-terephthylidene-bis(methyl-α-D-glucopyranoside) (**1**) is found to be a new LMOG. It gelatinizes only a limited number of solvents. Here, the gels of **1** with ethylene glycol (EG) and 1,3-propanediol (PG) are investigated with FT-IR, Raman, and UV–vis spectroscopies, the NMR relaxometry and diffusometry methods, and microscopic observation. The chemical structures of both solvents are closely related, but the variety of physical characteristics of the gels is large. The **1**/PG gels are thermally more stable compared to **1**/EG gels. The types of aggregates are most likely the H- and J-type in **1**/EG gels and the J-type in **1**/PG gels. Different microstructures are observed: bundles of crossing fibers for **1**/EG and a honeycomb-like matrix for **1**/PG gels. The diffusivity of the EG solvent in gels with **1** behaves as expected, decreasing with increasing gelator concentration, whereas the opposite behavior is observed for the PG solvent. This is a most fascinating result. To explain the diffusion enhancement, we suggest that a dynamic hydrogen bonding network of PG solvent in gel matrixes is disrupted due to solvent–gelator interaction. The direct proof of this interaction is given by the observed low frequency dispersion of the spin–lattice relaxation time of solvents in the gel matrixes.

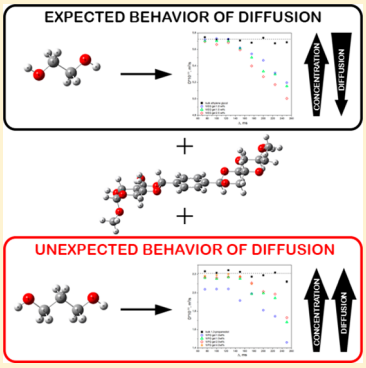

1. INTRODUCTION

The physical gels, particularly those based upon low-molecular-mass gelators (LMOGs), create an interesting class of soft materials with a wide variety of applications.[1,2] The LMOG-based gels are the subject of different studies, which allowed improvement of the understanding of the self-organization of gelator molecules into a three-dimensional network structure, the gelation phenomenon, and the dependence of the thermal stability and of gel morphology on the gelation.[3−24] However, some issues, e.g., concerning the interactions of solvent molecules with gelator aggregates during and after the gel formation, the role of solvent after the gel formation, and the influence of the gel matrix on the solvent dynamics, are still open for discussion. The above-mentioned problems were the subject of extensive studies.[14−22] The obtained results document the solvent–gelator interactions revealed by dispersion of the spin–lattice relaxation time of proton solvents measured in the gels as a function of the magnetic fields well. The solvent's influences on the physical properties of the gel during the gel formation are well documented in the literature, e.g., refs 6–14, 17, and 18. However, the attempt to correlate the thermal properties of the gel with different solvent parameters such as the dielectric constant, the one-component solubility parameter, the polarity parameter, or the Kamlet–Taft parameter is a difficult task. Studies have shown that such correlations are possible but apply only for a particular family of LMOG-based gels.[7−10,14,17,18] As to the role of solvent after the gel formation, we concluded in a recent paper[17] that the solvent plays only a passive role after gel formation. The conclusion was based on the similarity between the microstructure images observed for hydrazide-based gel and its xerogel.

In the LMOG-based gels, the gelator molecules self-assemble into the aggregates through hydrogen bonding, π–π stacking, van der Waals, London dispersion forces, or hydrophobic interactions.[1,2,23,24] The aggregates can have different morphologies like one-dimensional fibers, rods, ribbons, nanotubes, or two-dimensional objects like platelets.[1,2,23,24] To make gels, these objects have to further organize into three-dimensional networks, which immobilized the solvent component. Therefore, the LMOG gels can be treated as porous materials in which the solvent molecules are entrapped in the pores, spaces of a rigid, solid gel matrix.

The solvent dynamics in a gel matrix is an interesting phenomenon. Generally, liquids confined to pores show different physical properties than in the bulk. Enhancement of the correlation times by 6–8 orders of magnitude, and

Received: December 20, 2013
Revised: March 5, 2014
Published: March 17, 2014

   dx.doi.org/10.1021/jp412511e | *J. Phys. Chem. B* 2014, 118, 4005–4015

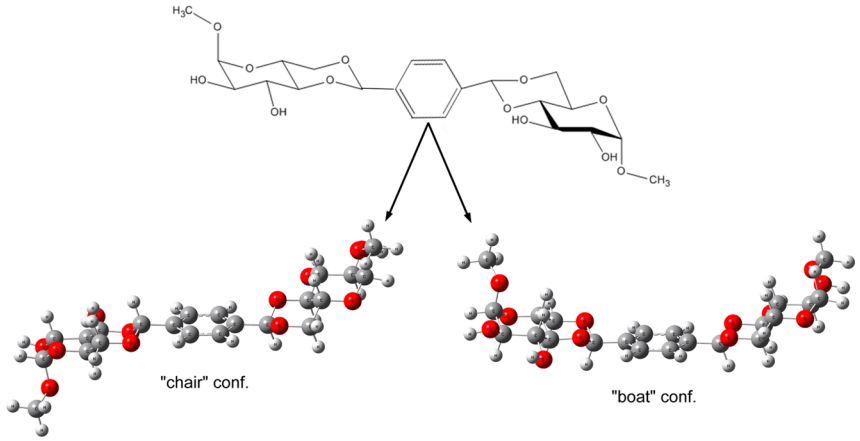

Figure 1. Optimized geometry of 4,6,4′,6′-*O*-terephthylidene-bis(methyl α-D-glucopyranoside) molecule obtained for the "chair" and "boat" conformations. The analysis of Raman spectra favors the "chair" conformation.

anomalous diffusion, as compared to bulk liquid, is observed together with the shifts of melting and freezing temperatures, and an orientational ordering of the liquid molecules at the pore surface.[25] All of these phenomena were observed in the LMOG-based gels.[15−17,20−22]

From a wide range of known LMOGs, sugar-based LMOGs have attracted significant attention because of their versatility in gelation and diversity of structures. Our previous experience with α-D-glucopyranoside[16,18,20] based organogelators stimulated us to investigate the more complicated glucopyranose derivatives as potential gelators. One of them is 4,6,4′,6′-*O*-terephthylidene-bis(methyl α-D-glucopyranoside) (**1**) composed of two glucopyrnoside units linked to a benzene core, as shown in Figure 1.

The compound was first designed and synthesized by Maślińska-Solich,[26] but its ability as a gelator has not been tested. This article is the first one which reports the gelation properties of **1**. From a wide variety of organic solvents tested, **1** formed stable gel only with glycerol, 1,3-propanediol (PG), and ethylene glycol (EG) solvents. Routinely, we started the studies with the determination of the energy minimized structure of **1**, the thermal properties of **1**/PG and **1**/EG gels, the aggregation mode of **1** in the gel fibers in these solvents, and the microstructure of gels. To continue our interest in the solvent−gelator interactions, we studied the solvent dynamics within the gel matrix of **1**. Different experimental techniques were employed in these studies including the FT-IR, Raman, and UV−vis spectroscopies, the NMR relaxometry and diffusometry methods, and microscopic observation. Despite the fact that the chemical structures of the PG and EG solvents are closely related, the variety of physical characteristics of the gels is large. The most intriguing result concerns the behavior of the diffusivity of PG solvent within the gel matrix of **1** observed as a function of gelator concentration. Therefore, in the interpretation of the experimental results, we focus on answering the question, why does the self-diffusion coefficient of the PG solvent increase with an increase of the gelator concentration and for 4 wt % of **1**/PG gel is much closer to the free bulk solvent than for 1 wt % of **1**/PG gel? We explained this diffusion enhancement as a result of the PG hydrogen bonding network disruption due to interaction of the solvent with the gelator aggregates.

2. EXPERIMENTAL SECTION

2.1. Material. 4,6,4′,6′-*O*-terephthylidene-bis(methyl α-D-glucopyranoside) (**1**) was synthesized according to the procedure described previously[26] (see the Supporting Information).

2.2. Gel Preparation. The gels are prepared from mixtures of powdered gelator **1** and a proper solvent under different weight concentrations of gelator ranging from 0.1 to 5% (wt %) via a thermal heat−cool cycle, which allows the formation of the noncovalent interactions responsible for the gel network. Upon cooling below a characteristic temperature T_{gs}, the sol is converted into an elastic gel that can hold its weight under the "tube inversion test". The gelation behavior of **1** in 40 solvents of different polarity was tested at a concentration of 3 wt %, and the results are shown in Table 1 of the Supporting Information.

2.3. Determination of the Gel−Sol Phase Transition Temperature (T_{gs}). The temperature was determined by the air-bath method and visual inspection of the samples. For this purpose, an experimental setup was designed and built to allow direct observation of the gel phase. The setup comprises a glass tube with a holder which allows tilting the whole setup at angles from 0 to 60° off the perpendicular (off plumb) to facilitate the observation of changes in the gels. Within the glass tube, a glass dewar is placed with a heater and an inlet of cooling gas (dry gaseous nitrogen), besides some Teflon spacers and grills to ensure homogeneous mixing of the gas and equal distribution of temperature in the sample volume. The temperature of the gas was controlled by VTC to an accuracy of ±0.1 K. The T_{gs} temperature was determined upon heating the sample to a temperature at which the system starts to flow.

2.4. FT-IR, Raman, and UV−vis Spectroscopies. The vibrational spectra of the gelator molecule were investigated at room temperature using Raman scattering and absorption techniques. The Raman spectra of the polycrystalline sample in the range from 100 to 4000 cm^{-1} were investigated with a Jobin Yvon HORIBA LabRAM HR 800 confocal spectrometer with a liquid-N_2-cooled charge couple device (CCD) and Stabilite 2017 argon ion laser (λ_{laser} = 514 and 488 nm). The laser power before focusing with the objective was less than 7 mW. The spectral resolution of Raman spectra was better than 2 cm^{-1}. Absorption spectra were collected using a FT-IR Bruker Equinox 55 spectrometer within the spectral region from 400 to 7000 cm^{-1} with a resolution of 2 cm^{-1}. Additionally, we studied the absorption electronic spectra (UV−vis) of gelator **1** in KBr

dx.doi.org/10.1021/jp412511e | J. Phys. Chem. B 2014, 118, 4005−4015

pellets and in solutions of PG and EG solvents, in the spectral region from 190 to 1100 nm using a Hitachi U2900 spectrometer.

2.5. Computational Methods. To interpret intramolecular excitations in the electronic spectra and vibrational transitions, the quantum-chemical calculations were carried out following a two-step procedure: the optimization of the ground-state geometry with the B3LYP theory level using a basis set 6-31++G(d,p) and the determination of the electronic transition energies by means of TD-B3LYP/6-31++G-(d,p).[27−29] The 200 singlet−singlet electronic transitions were computed by applying the time-dependent DFT approximation[30] to their correspondingly optimized ground-state geometries. Calculations were made on a single molecule using the Gaussian 03 program package.[31] The vibrational transitions were performed at the B3LYP theory level using the basis set 6-31++G(d,p) where the B3LYP functional includes a mixture of HF exchange with DFT exchange correlation, given by Becke's three-parameter functional[32,33] with the Lee, Yang, and Parr correlation functional.[34] The computed frequencies were scaled using the factor 0.9614 to eliminate known systematic errors, correcting the anharmonicity.[35] The mode description was performed by visual inspection of the individual modes using the Gauss View program. Moreover, the theoretical Raman intensities were calculated from scattering activities and calculated wavenumbers obtained from the Gaussian calculations.[36−38]

2.6. Microscopic Observation. The gel microstructures were taken by an Olympus BX53 microscope (Japan) and Olympus Stream START software used for recording and analyzing obtained images. The configuration of the system allowed for observation with the use of phase contrast mode, differential interface mode, and polarizing mode which allowed visualizing molecular aggregates of the gelator. The images were obtained for a gel sample carefully cast on the microscopic slides covered with a 130 μm coverslip and immediately subjected to microscopic observations.

2.7. NMR Diffusion Experiment. NMR diffusion measurements were performed with a Bruker Avance II spectrometer operating at 300 MHz for protons and coupled with a 7.1 T, 89-mm-bore Bruker magnet. The system is equipped with a Micro 2.5 probehead and a gradient system capable of producing pulse gradients up to 1 T m^{-1} in each of the three perpendicular directions. The NMR glass tube of 8 mm with a particular gel or solvent was placed inside a 10 mm RF coil and aligned along the z direction in the magnet. The conventional pulse gradient spin echo (PGSE) methodology[39] was applied for measuring diffusion of pure solvents and solvents confined in the cavities of gels of **1**. The PGSE signal is phase encoded according to the molecular displacement over a Δ diffusion time. The molecular displacement leads to an attenuation of the echo signal, which is related to the experimental parameters by the relation[39]

$$\frac{A(g)}{A(0)} = \exp\left[-\gamma^2 g^2 \delta^2 D\left(\Delta - \frac{\delta}{3}\right)\right] \quad (1)$$

where $A(g)$ and $A(0)$ are echo signal intensities with and without magnetic field gradient pulse applied, γ is the gyromagnetic ratio of the nucleus studied, and D is the self-diffusion coefficient. The echo signal intensity was measured as a function of g. For free diffusion, a plot of $\ln(A(g)/A(0))$ against $b = \gamma^2 G g^2 \delta^2(\Delta - \delta/3)$, the so-called Stejskal−Tanner[39] plot, produces a straight line whose slope represents the diffusion coefficient D. In some cases, a curvature in the Stejskal−Tanner plot is observed that may result from multiple components, i.e., species diffused in inhomogeneous porous material. In this case, a stretched exponential function (given by modification of eq 1, in which the expression in square parentheses is raised to β) can be applied for the description of the echo decays in order to yield D_{app} (the apparent diffusion coefficient) values.[40−43] The β parameter in the modified eq 1 describes the distribution of diffusion coefficients. In our experiment, the pulse gradient was applied in the z direction and varied in 32 steps from 0 to a maximum value of 1 T m^{-1}. The parameter δ was equal to 2 ms. The diffusion coefficients for bulk PG and EG solvents and these solvents in the gels of **1** were studied as a function of Δ in the range from 70 to 250 ms, and as a function of gelator concentration from 1 to 4 wt %. The measurements were carried out at 290 K. Because of a low concentration of gelator molecules and rigidity of the gel matrix, the measured NMR signal originates only from solvent protons.

2.8. NMR Relaxometry Measurements. The spin−lattice relaxation times T_1 of protons (^{1}H) of bulk solvents and solvents in gels made with **1** were measured on a SpinMaster 2000 field cycling (FC) relaxometer from Stelar Company, Mede, Italy, which covers the proton frequencies from 0.01 to 40 MHz. The measurements were performed as a function of the magnetic field B_0 but expressed in terms of proton Larmor frequency. The plot of the relaxation rate R_1 ($R_1 = 1/T_1$) vs Larmor frequency is called the nuclear magnetic resonance dispersion (NMRD). The technical details of the FC NMR relaxometry experiment are reported elsewhere.[25,44,45] The magnetization measured in the gels comes only from the solvent protons because the contribution of the gelator aggregate protons, which form a rigid matrix in the gel phase with strongly restricted motion, is undetectable under the applied NMR measuring conditions. Because of the low resolution of FC NMR relaxometry measurements and the inhomogeneity of the magnetic field, the resonances of OH and CH_2 groups of PG and EG solvents totally overlapped. The measurements were performed at 290 K corresponding to the gel phase. The temperature of the sample was controlled by VTC and stabilized within ±0.01 K accuracy.

3. RESULTS AND DISCUSSION

3.1. Gelation Properties. Gelation tests were carried out using solvents of different polarity (Table 1 of the Supporting Information). The macroscopic behavior of the obtained materials was initially analyzed by monitoring the transition from an immobile to a mobile self-assembly state using "the tube inversion test". This simple method is widely used to evaluate the gel formation of low-molecular-mass gelators. With reference to Table 1 (Supporting Information), it can be concluded that the gelation processes were observed among tested solvents only for glycerol, ethylene glycol (EG), and 1,3-propanediol (PG). The gels of **1** with the two latter solvents were the subjects of our studies. The gels are thermoreversible and opaque, and remained stable for several months at room temperature. Their thermal stabilities defined by the gel melting temperature T_{gs} were analyzed as a function of the gelator concentration. In Figure 2, plots of T_{gs} as a function of the organogelator **1** concentration (w/w, %) are shown.

Organogels formed by **1** with PG are more stable than those formed with EG, as accounted for by the T_{gs} value—the

dx.doi.org/10.1021/jp412511e | J. Phys. Chem. B 2014, 118, 4005−4015

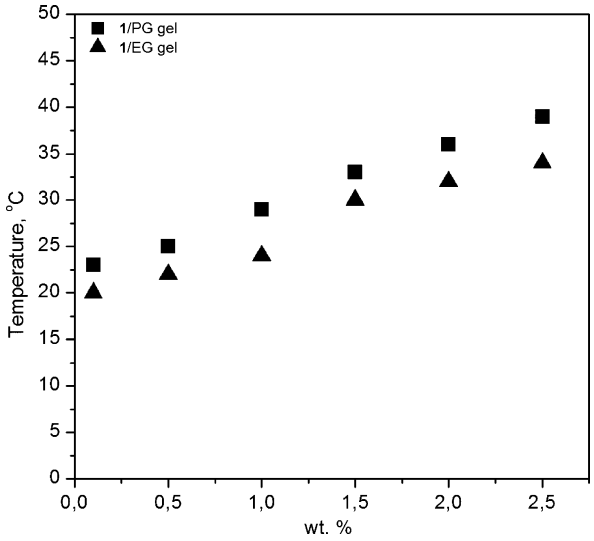

Figure 2. Plots of T_{gs} versus the organogelator **1** concentration (w/w, %) in ethylene glycol and 1,3-propanediol.

temperature continuously increases as a function of gelator concentration being for each of the concentrations higher for **1**/PG gel as compared to **1**/EG gel. The gel−sol phase transition temperatures were determined for "fresh" gels within 24 h after preparation. We noticed that, despite the fact that these gels undergo the usual inverse tube gel test, they evolve toward equilibrium state for much longer times. The T_{gs} values determined after 2 weeks from the first measurements were higher by about 20° C for each of the studied gelator concentrations. All NMR and microscopic measurements were done for samples at equilibrium state. Due to the sample preparation procedure for FT-IR, Raman, and UV−vis measurements, the nonequilibrated samples were investigated. However, we expect that this fact influences only the values but not the phenomenon itself (please refer to the Supporting Information for an explanation).

3.2. Characterization of Gelator Molecule. The "boat" and "chair" conformations of the gelator **1** molecule have been taken under consideration in our studies. The fully optimized geometrical structures of these conformations are presented in Figure 1. The normal-mode analyses were carried out for both optimized structures. For these structures, no imaginary frequencies have been observed. In Figure 3, the FT-IR (a) and Raman (b) spectra of the investigated gelator **1** are shown together with the corresponding theoretical spectra (B3LYP/6-31++G(d,p)) given for comparison.

The analysis of the selected normal modes of the studied compound is given in Table 2 of the Supporting Information. The assignment is based on the comparison of calculated and experimental absorption and Raman spectra. According to the normal-mode analysis, the gelator **1** molecule has 186 fundamental intramolecular vibrational modes. The match between the simulated and experimental spectra for the investigated compound is fairly good. It shows that the applied model, which neglects the intermolecular interaction, can be used for the studied material. Moreover, the analysis of normal modes allows the proposing of marker bands that can be useful for the determination of the conformation of the gelator. In Figure 3, using the asterisk symbol, we denoted bands characteristic of the "boat" conformation. It is well-known that stretching bands may be applied as diagnostic features for recognition of conformation. The intensity and position of the calculated modes are dependent on the type of conformation. In order to be sure that the intensities of these bands are independent from the excitation energy of light, we also analyzed the Raman spectra for two laser excitation lines: 488 and 514 nm (Figure 4). No significant intensity changes in experimental spectra were observed. This leads us to conclude that the resonance Raman scattering effect is not present for the gelator **1** molecule. These observations convinced us to suggest that the most probable conformation for the gelator is the "chair" conformation.

3.3. Characterization of the Aggregation Mode Responsible for Gelation. The chemical composition of **1** (Figure 1) suggests that the intermolecular H-bonding of the sugar part together with the intermolecular $\pi-\pi$ interaction between benzene are the driving forces for gelator **1** molecules to aggregate. The polar solvent molecules usually act as competing hydrogen-bond donors and acceptors and therefore

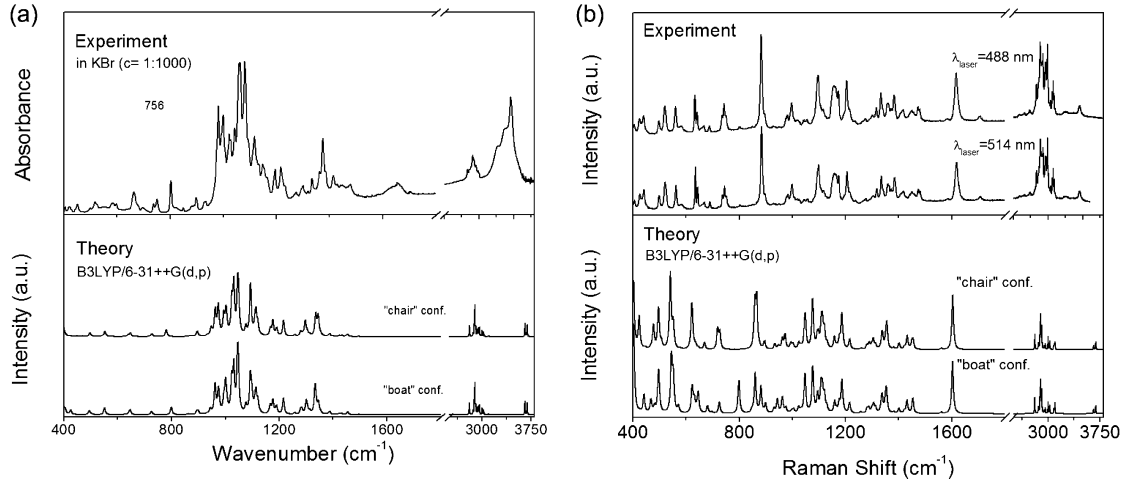

Figure 3. Experimental and calculated FT-IR spectra of gelator **1** molecule recorded in KBr matrixes (c = 1:1000) (a). Experimental and calculated Raman spectra of gelator **1** molecule (b). Note: the experimental Raman spectra were recorded with 488 and 514 nm excitations; the simulated spectra were obtained for "boat" and "chair" conformations at the theory level B3LYP/6-31++G(d,p) (the spectra were scaled using the 0.9613 scaling factor); ν means stretching and δ bending vibrations.

dx.doi.org/10.1021/jp412511e | J. Phys. Chem. B 2014, 118, 4005−4015

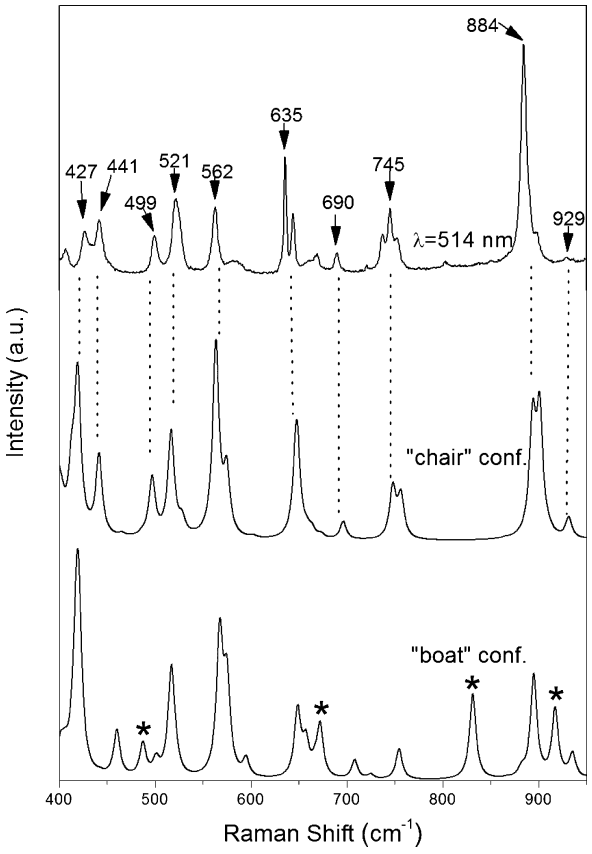

Figure 4. Experimental Raman spectra of gelator **1** molecule recorded with λ = 514 nm excitation together with calculated spectra obtained for "boat" and "chair" conformations of molecule at the theory level B3LYP/6-31++G(d,p) (unscaled data). Note: the dotted lines are used as a guide to the eye; the asterisk symbol (*) denotes bands characteristic of the "boat" conformation.

suppress the self-aggregation mechanism based on the hydrogen-bonding interaction. The PG and EG are the polar liquids. Moreover, it is well recognized that ethylene glycol is a strongly hydrogen bonding liquid, whose molecules form multiple hydrogen bonds to yield a network-like structure.[46,47] Therefore, we can assume that the functional OH groups of EG molecules participate in the hydrogen bonding network and will not compete with the gelator−gelator hydrogen bonding interactions. As for the 1,3-propanediol, the situation is not so clear. Tavernier et al.[46] showed that the electron transfer data in 1,3-propanediol can be fitted with the single molecule radial distribution function with diameters of the single solvent molecules of 4−5 Å, whereas for ethylene glycol the fit can be done only with a radial distribution function in which the effective solvent size is about 17 Å. These results can suggest that PG is the "normal", not aggregated, solvent in contradiction with the aggregated EG solvent. On the other hand, Usacheva at al.,[48] in order to interpret the dielectric spectra of PG, had to assume that the molecules formed the dynamic hydrogen bonding clusters with different sizes and shapes. Therefore, for **1**/PG gel, hydrogen bonding interactions cannot be ruled out as a driving force for gelation in addition to the $\pi-\pi$ stacking interaction.

The insight into the aggregation mode for gelator **1** molecules in the gel fibers was obtained by UV−vis spectroscopy. The electronic spectra of the gelator molecule dissolved in EG and PG solvent (concentration of 0.0022 wt %) are shown in Figure 5a. They are similar to each other and show two absorption maxima at about 191 nm (denoted as A) and 225 nm (band B). In order to interpret the experimental data, the properties of the ground and excited states of compound **1** molecule were investigated. For "boat" and "chair" conformations of the gelator molecule, the energy levels have been calculated and for the latter conformation are presented in Figure 4 of the Supporting Information. The energy of the highest occupied molecular orbital (HOMO) is equal to −6.61 eV for both conformations, whereas the lowest unoccupied molecular orbital (LUMO) is −0.60 eV and −0.61 for "chair" and "boat" conformations, respectively. The DFT calculations give a very similar HOMO−LUMO energy gap (ΔE = 6.0 eV) for both considered conformations.

To assign the transition bands of gelator **1** in EG and PG solvents (Figure 5), the characterization of electronic transitions was further performed using the time-dependent

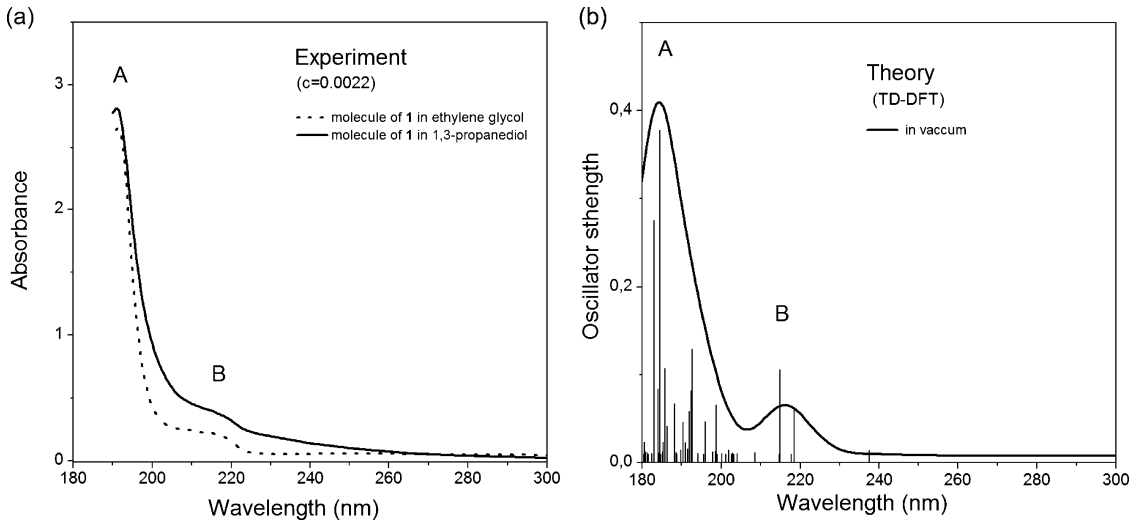

Figure 5. Experimental UV−vis absorption spectra of gelator **1** molecule dissolved in ethylene glycol (dotted line) and in 1,3-propanediol (solid line) (a). Vertical transitions for the first 200 excited states calculated using TD-DFT and the corresponding simulated electronic spectrum performed for the "chair" conformation (b).

dx.doi.org/10.1021/jp412511e | J. Phys. Chem. B 2014, 118, 4005−4015

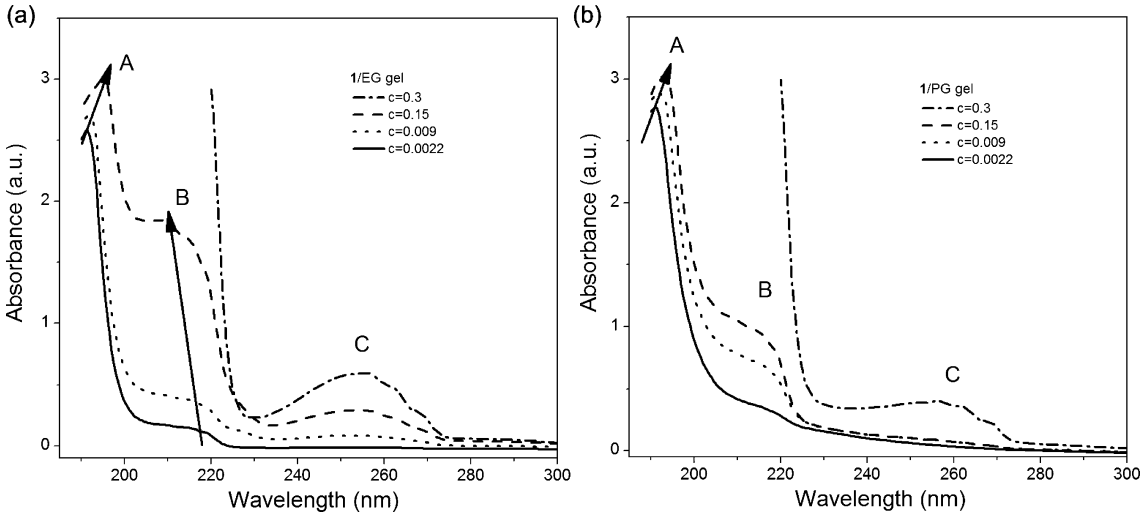

Figure 6. Experimental UV−vis absorption spectra of gelator **1** molecule studied as a function of gelator concentration in ethylene glycol (a) and in 1,3-propanediol (b). The concentration 0.3 wt % corresponds to the gel phase.

DFT method on their correspondingly optimized ground-state geometries. The results of the theoretical calculations performed for the "chair" conformation of compound **1** are compared with experimental measurements in Figure 5 and in Table 3 of the Supporting Information. The theoretical transitions reported in the following correspond to the singlet excited states with dipole allowed transitions (i.e., nonzero oscillator strength) from the ground state. A graphical representation of the orbitals at play for electronic transitions is given in Figure 4 of the Supporting Information. As can be seen from Table 3 of the Supporting Information, the electronic bands observed at about 190 and 218 nm are due to the superposition of many transitions, but the latter one is predominantly related to HOMO → LUMO and HOMO → LUMO+2. Generally, we can conclude that the theoretical calculations at the TD-B3LYP/6-31++G(d,p) level of theory show that the transition bands of **1** in EG and PG solutions (Figure 5) are due to the electronic excitations predominantly connected with π(benzene) → π^*(benzene) and charge-transfer (CT) transitions. The excitation of electrons from the benzene to the outer part of the gelator molecule plays the role in creating CT transition.

To monitor the interaction between the gelator **1** molecules during the formation of the gels, absorption spectra of compound **1** in PG and EG solvents were investigated as a function of gelator concentration and are shown in Figure 6.

The concentration 0.3 wt % corresponds to the gel phase. The spectra revealed different behavior of self-aggregation of gelator molecules in EG and PG solvent. Compared with the sols, a shift of the maximum of the absorption peak A (λ_{max} = 191 nm) to higher wavelengths can be detected for two gels and is equal to 4 and 2.5 nm for **1**/EG and **1**/PG gel, respectively. The shift of the maximum of the absorption peak B (λ_{max} = 218 nm) is observed only in **1**/EG gel and occurs to lower wavelengths by about 8 nm. By comparing the spectra of the gelator in dilute solution to those obtained in the gel state, the nature of the self-assembled aggregates formed in the gel phase can be established to be either the H- or J-type.[49−51] The red-shifted spectral features suggest that the J-type nanostructures are more likely to be formed in the self-assembled aggregates, whereas the blue-shift indicates the H-aggregation mode. Therefore, presumably in ethylene glycol, the molecules **1** formed H- and J-type of aggregates, whereas in 1,3-propanediol J-type nanostructures are more likely to be formed in the self-assembled aggregates.

The differences in the self-aggregation behavior of gelator **1** in EG and PG solvent are additionally observed through concentration dependent on the absorption band C observed in the spectrum of **1** at about 255 nm in EG and at 260 nm in PG. This band is not visible in spectra of **1** in both solvents at a gelator concentration of 0.0022 wt % (noninteracting gelator molecules). Therefore, its appearance is attributed somehow to the gelator−gelator interaction, which leads to gelator aggregation followed by growth of the fibers and finally to the formation of gel. In EG, this interaction occurs already at a gelator concentration of 0.009 wt % reflected by the appearance of a corresponding absorption band, whose amplitude increases as a function of gelator concentration. Therefore, EG molecules being involved in the hydrogen bonding network between them does not suppress the self-assembling process of gelator molecules. Contrary to EG molecules, the PG molecules seem to interact with gelator molecules during the gel formation and therefore are competing with gelator−gelator interactions. As a result, the band C is appearing at higher gelator concentration and its amplitude is increasing much slower as compared to band C of the spectrum of **1**/EG. When plotted the integral intensities of corresponding C bands against concentration (Figure 5 of the Supporting Information) it is clearly seen that the results in ethylene glycol differ from that in 1,3-propanediol.

3.4. Gel Microstructure. The studied gels were analyzed in their gel phase by microscopic observation to reveal the supramolecular assembly of the gelator aggregates with PG and EG solvent still trapped inside gels. The optical micrographs of wet **1**/EG and **1**/PG gels are shown in Figure 7.

It is seen that the different behavior of self-aggregation of gelator **1** molecules in PG and EG solvents is also reflected in different microstructures of studied gels. The matrix of **1**/EG gel consists of bundles of crossing fibers with different lengths, and orientations, dispersed in the gel. The matrix of **1**/PG gel is much more regular and appears like a honeycomb. The latter supermolecular network clearly depicts the better entrapment of the solvent molecules as compared to the **1**/EG gel.

dx.doi.org/10.1021/jp412511e | J. Phys. Chem. B 2014, 118, 4005−4015

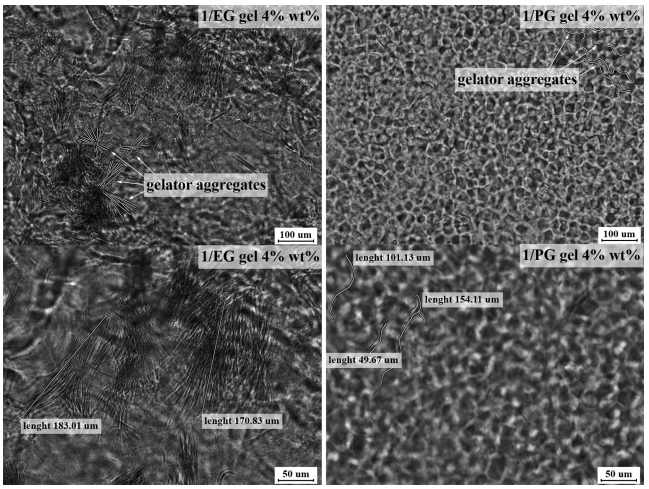

Figure 7. Microscopic images of the microstructure of **1**/EG gel (left) and **1**/PG gel (right).

3.5. Diffusion of PG and EG Solvents in Gel Matrixes of 1. The ^{1}H PGSE NMR technique has been successfully applied in the observations of diffusion behavior of small molecules of a liquid entrapped in gel phase,[20,52,53] and therefore, it was used by us to study the solvent diffusion in gels composed by **1** with EG and PG and free bulk solvents, for comparison. The measured diffusion coefficients showed the dependence on gelator concentration and on the diffusion time Δ (Figure 8). They were estimated with the same analysis.[39,40] The data on Stejskal–Tanner[39] plots were fitted with eq 1 for bulk solvents and solvents in the gels in the range from 60 to 130 ms. For larger values of Δ, the stretched exponential function (modify eq 1)[40,53] was applied for fitting the echo decays in order to yield D_{app} values.

For bulk PG and EG, all the data obtained with different diffusion times are on a straight line. This indicates that the diffusion coefficients of the solvents and their diffusion behavior are not changing within the diffusion time. The plots in Figure 8 show that for bulk PG the diffusion coefficient is lower than those of pure EG. The values are correspondingly equal to 2.23 × 10^{-11} and 5.72 × 10^{-11} m^2/s. The differences are mostly due to the viscosity values which differ very much for both solvents and are equal at 25 °C to 16.1 mPa for EG and 40.4 mPa for PG. The diffusion coefficients of EG and PG solvents in gel matrixes of **1** showed a similar Δ dependence. Their values are lower than those of the corresponding bulk solvents (especially for PG solvent) and in the range of 60–130 ms are independent of the diffusion time. The lower values of D_{app} are indicative of the restricted diffusion of EG and PG solvents inside the pore spaces of the corresponding gel matrixes of **1**. The independence of D_{app} on Δ means that restricted diffusion takes place inside the pore space over the length scale that is much smaller than the root-mean-square displacement of the bulk solvents. It is interesting to compare the D_{app} values for **1**/EG and **1**/PG of 1 wt % gels with corresponding values for bulk solvents. A slowing down of the diffusion of PG molecules occurs in the gel (2.03 × 10^{-11} m^2/s as compared to 2.23 × 10^{-11} m^2/s), whereas the D_{app} of EG in the 1 wt % gel is close to that of the bulk solvent (Figure 8). This means, at least apparently, that obstruction by the **1**/EG gel network becomes much less significant than that for **1**/PG, and that there are pores within the **1**/EG gel matrix big enough in diameter that almost unrestricted diffusion takes place for the shortest values of the diffusion time. Such results correspond well with the microstructure of the studied gels. With increasing diffusion time (in the range 140–250 ms), the decrease of D_{app} is observed for both gels and all studied concentrations. It is typical of restricted diffusion of the solvent molecules diffusing inside the pores of gel over the length scale that is of an order of the pore diameter. In this regime, the root-mean-square displacement does not increase any more with time and thus D_{app} is expected to decrease with Δ.[53] The character of the decrease of D_{app} in the whole diffusion time range as shown in Figure 8 is typical of restricted diffusion in pores and is very similar to the theoretical one predicted for molecular diffusion restricted in spherical pores.[53]

Contrary to the similar Δ dependence, the diffusion coefficients of EG and PG solvents in gel matrixes of **1** show the opposite concentration dependence. The D_{app} of EG decreases as a function of gelator concentration, whereas the decrease of D_{app} of PG is observed only at the lowest gelator concentration (1 wt %) following the increases of diffusion

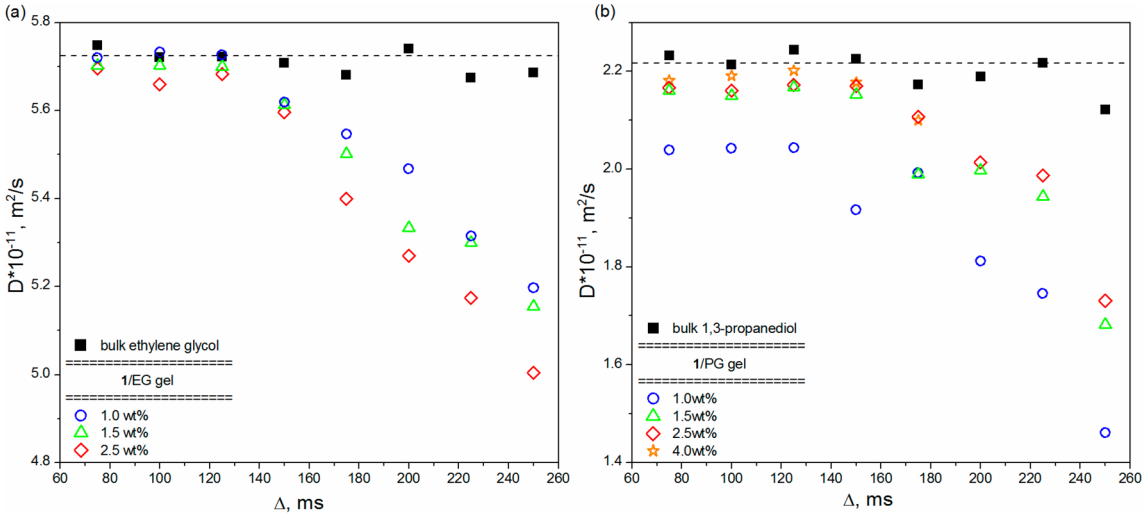

Figure 8. The diffusion coefficients D_{app} of ethylene glycol (a) and 1,3-propanediol (b) in the gel matrixes of gelator **1** studied as a function of the diffusion time Δ and gelator concentration. For comparison, the diffusion coefficient data for bulk solvents are also given.

dx.doi.org/10.1021/jp412511e | J. Phys. Chem. B 2014, 118, 4005–4015

coefficient with further increase of gelator concentration (from 1.5 to 4 wt %). The measurements for **1**/PG gel were repeated a second time to check for reproducibility, giving the same results. It is well established that the increase of gelator concentration leads to a decrease of diffusion mobility of solvent in gel. Therefore, the behavior observed for PG is somehow intriguing. This presents us with an interesting question: why does the diffusion coefficient of the PG increase with an increase of the gelator concentration and for 4 wt % gel is much closer to the free solvent value than for 1 wt % gel?

We postulate that the explanation of this is connected to the molecular structure of the solvent. 1,3-Propanediol has 67% of carbons bound to OH, and every molecule of PG has a methyl group. Therefore, in the hydrogen bonding network formed by PG molecules, the vicinity of the methyl groups in the network can provide the needed defect size, necessary to make possible the interaction of gelator aggregates with the PG molecules. As a consequence of gelator−solvent interaction, a dynamic hydrogen bonding network of 1,3-propanediol in the gel matrix is disrupted or broken down to some extent. Solvent aggregates become smaller in size and diffuse faster with the diffusion coefficient value much closer to the free liquid value. We assume that the microstructure of **1**/PG gel is not changing significantly with increasing gelator concentration, as proved by NMR relaxometry data.

Ethylene glycol formed an extended hydrogen bonding network[46] but in contrast to 1,3-propanediol has 100% of its carbon bound to an OH. Therefore, there are no defect sizes in the network, the effective solvent size is large, and gelator aggregates have difficulties inserting into such a network, and disrupt it.

3.6. Evidence of the Solvent−Gelator Interactions by Dispersion of the Relaxation Time of Solvents. The FC NMR relaxometry method gives relaxation data acquired over a wide time scale and therefore is sensitive to molecular motions in a wide range of frequency including slow motion. Thus, it is well suited for determination of the dynamics of solvent in porous media. Recently, this method was applied with success to organogels for the study of the spin−lattice relaxation time of solvent within the gel matrix which allows to directly probe the interaction of the solvent with the gelator aggregates.[15−17,21,22] This interaction is manifested by the dispersion of the spin−lattice relaxation time of the solvent in the low frequency range, below 10^6 Hz.

Herein, the relaxometry measurements were performed to obtain the information about the interaction of PG and EG solvents with gelator **1** aggregates. Figure 9 presents the NMRD profile of 1,3-propanediol in **1**/PG gel and of ethylene glycol in **1**/EG gels together with the corresponding profiles for bulk solvents. The observed difference in the relaxation rate R_1 of bulk PG and EG solvents is mainly due to the viscosity values. The larger viscosity of PG solvent means slower molecular motions, stronger dipole−dipole couplings being the main spin−lattice relaxation mechanism for protons,[54] and consequently gives shorter T_1 (or longer R_1) as compared to EG solvent. Slower dynamics of PG causes a shift of the frequency at which the maximum dispersion occurs (the so-called inflection point) to a lower value (about 8 MHz) compared to EG (well above 20 MHz). The NMRD profiles of bulk PG and EG solvents are frequency independent in the low frequency region below 1 MHz. In contrast, below 1 MHz, a broad and pronounced dispersion region (smooth increase of R_1 with decreasing frequency) appears in R_1 for PG and EG in

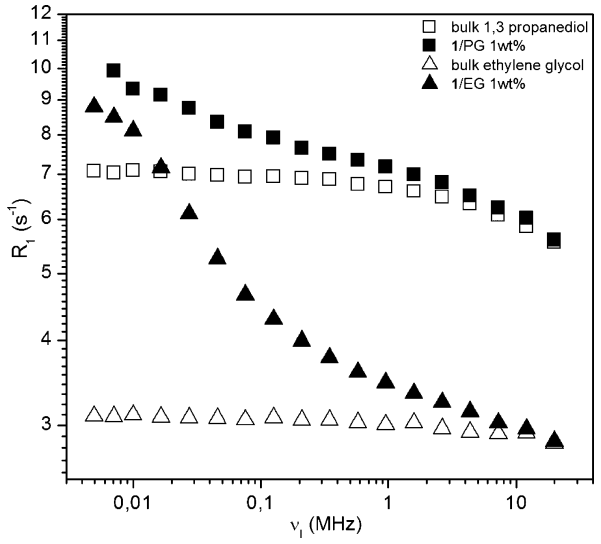

Figure 9. NMRD profile of 1,3-propanediol in **1**/PG gel and of ethylene glycol in **1**/EG gel at 290 K, together with the corresponding profiles of bulk solvents.

the gel phase. The observed low frequency dependence of NMRD profiles, as described previously,[15−17,21,22] is therefore a fingerprint of a specific interaction experienced by EG and PG solvents in the presence of a rigid structure of gelator aggregates.

To get better insight into the solvent−gelator interactions, the relaxometry measurements were performed for both solvents in corresponding gels of **1** as a function of gelator concentration in a range from 0.25 to 4 wt %. The obtained NMRD profiles are shown in Figure 10.

The measured R_1 values of solvents in the gel phase at each frequency and for all gelator concentrations were divided by the corresponding values of R_1 obtained for bulk solvent and additionally normalized for the corresponding R_1 values at 20 MHz. Therefore, the low frequency dispersion of NMRD profiles shown in Figure 10 reflects only the solvent−gelator interactions without a possible contribution from intermolecular dipole−dipole coupling.[55] For **1**/EG gel, the amplitude of the dispersion continuously increases as a function of the gelator concentration. The increase of the concentration corresponds to the increase of the matrix surface interacting with the EG aggregates and consequently to the increase of the solvent−gelator interaction, which leads to the slowing down of the EG solvent. As a consequence, the diffusivity of the solvent in **1**/EG gel decreases with an increase of gelator concentrations. Thus, the relaxometry results coincide with the diffusometry ones.

The concentration dependence of the dispersion for **1**/PG gel is different from that for **1**/EG gel. The continuous increase of the amplitude of dispersion is observed only for **1**/PG gels up to 1.5 wt % followed by a small decrease of the dispersion for 2 wt % gel and finally almost no dependence on the concentration is observed for gels with higher concentrations. Such behavior is somewhat confusing because with the increase of the gelator concentration the solvent−gelator interactions reflected by the amplitude of the NMRD should increase instead of being almost constant. To explain this, we suggest that for **1**/PG gel the solid matrix of the gel composed of the gelator aggregates can develop only to some extent. Above a particular gelator concentration (2 wt %), the gelator molecules

dx.doi.org/10.1021/jp412511e | J. Phys. Chem. B 2014, 118, 4005−4015

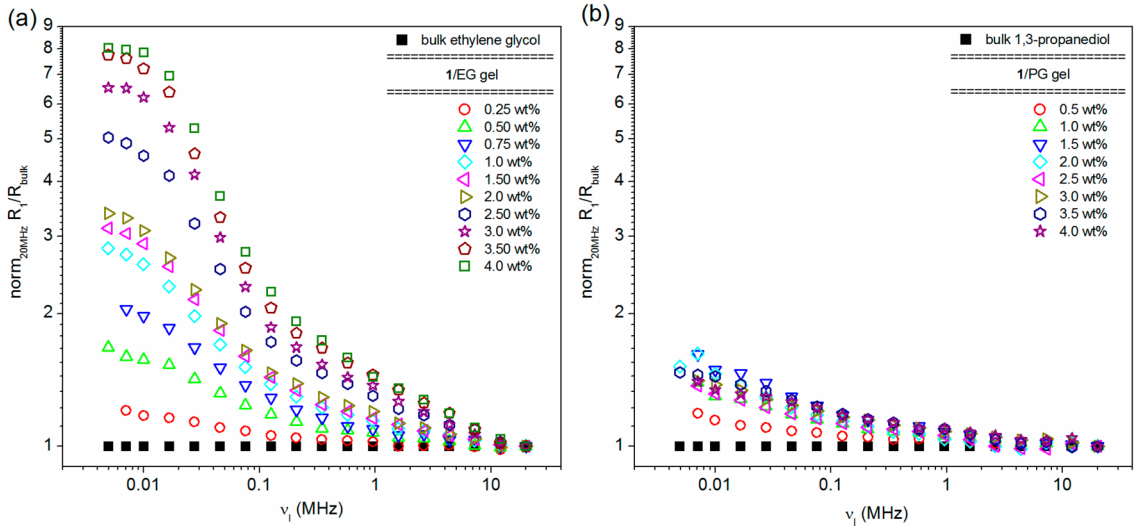

Figure 10. Normalized NMRD profiles for EG (a) and PG (b) solvents in corresponding gels of **1** as a function of gelator concentrations.

are not forming a further gel matrix but are interacting with PG aggregates, leading to their disruption. As a result, the microstructure of the gel matrix remains unchanged but the size of the solvent aggregates decreases. As a consequence, the increase of the solvent diffusivity is observed for higher gelator concentration, as indicated by the measured diffusion coefficients.

A more detailed analysis of the relaxometry data will be given in a separate paper because they are not necessary for the purpose of this work.

4. CONCLUSIONS

In this paper, we disclose gelatinized properties of 4,6,4′,6′-*O*-terephthylidene-bis(methyl-α-D-glucopyranoside) compound. This new LMOG formed gels only with a very limited number of solvents, among them PG and EG solvent. They are similar solvents, common polyether diols, with similar chemical formulas and shapes of molecules. Thus, we expected that the gels of **1** with PG and EG solvents will be characterized by related properties. Contrary to this expectation, the results have shown that **1**/PG and **1**/EG gels are different. They differ as to the thermal stability and aggregation mode of gelator **1** molecules, as shown by UV−vis spectroscopy. Consequently, a different microstructure of both studied gels is observed. Thanks to the PGSE and relaxometry measurements, we were able to probe and show the differences of the dynamics of hydrogen-bonding networks of PG and EG solvents in the gel matrixes of **1**, being the consequence of different ways of interaction of these solvents with the same gelator **1**. In **1**/EG gels, the gelator interacts with solvent aggregates without causing their disruption, whereas the gelator−solvent interaction in **1**/PG gels breaks up the intermolecular hydrogen bonding forces of the 1,3-propanediol results in a disruption of its aggregates. We assumed that the latter phenomenon is the main factor influencing the diffusion of 1,3-propanediol in gel matrixes of **1**, and is responsible for the observed enhancement of the diffusion coefficient observed for gel with a higher concentration relative to gel with **1** wt %. The enhanced diffusivity was previously observed for diols that diffuse in porous media.[56]

In the molecular gels, the question about the solvent−gelator interaction is one of the most important and still open for discussion. We believe that the presented results shed new light on this interaction.

The interesting results concern the solvent effect. The studies presented have shown that even the same type of solvent, diols, can affect in a different way the aggregation mode of the same gelator and consequently further the properties of gel.

■ ASSOCIATED CONTENT

Ⓢ Supporting Information

Description of nonequilibrated samples, ^{1}H and ^{13}C spectra of compound **1**, the energy levels of molecule **1** in "chair" conformation and their graphical representation, gelation test of **1** with 40 solvents, and the theoretical analysis of selected modes of FT-IR and Raman spectra. This material is available free of charge via the Internet at http://pubs.acs.org.

■ AUTHOR INFORMATION

Corresponding Author

*Phone: +48 61 8695 226. E-mail: jtg@ifmpan.poznan.pl.

Notes

The authors declare no competing financial interest.

■ ACKNOWLEDGMENTS

Financial support for this work was provided by the National Centre for Science (Grant No. N202 1961 40).

■ REFERENCES

(1) Terech, P.; Weiss, R. G. *Molecular Gels. Materials with Self-Assembled Fibrillar Network*; Springer: Dordrecht, The Netherlands, 2006.

(2) Liu, X. Y.; Li, J. L. *Soft Fibrillar Materials: Fabrication and Applications*; Wiley-VCH Verlag GmbH & Co.: Weinheim, Germany, 2013.

(3) Xu, Z.; Peng, J.; Yan, N.; Yu, H.; Zhang, S.; Liu, K.; Fang, Y. Simple Design but Marvelous Performances: Molecular Gels of Superior Strength and Self-healing Properties. *Soft Matter* **2013**, *9*, 1091−1099.

(4) Samai, S.; Dey, J.; Biradha, K. Amino Acid Based Low-Molecular-Weight Tris(bis-amido) Organogelators. *Soft Matter* **2011**, *7*, 2121−2126.

(5) Allix, F.; Curcio, P.; Pham, Q. N.; Pickaert, G.; Jamart-Gregoire, B. Evidence of Intercolumnar π−π Stacking Interactions in Amino-

Acid-Based Low-Molecular-Weight Organogels. *Langmuir* **2010**, *26*, 16818−16827.
(6) Makarevic, J.; Jokic, M.; Peric, M.; Tomisic, V.; Kojic-Prodic, B.; Zinic, M. Bis(Amino Acid) Oxalyl Amides as Ambidextrous Gelators of Water and Organic Solvents: Supramolecular Gels with Temperature Dependent Assembly/Dissolution Equilibrium. *Chem.—Eur. J.* **2001**, *7*, 3328−3341.
(7) Zhu, G.; Dordick, J. S. Solvent Effect on Organogel Formation by Low Molecular Weight Molecules. *Chem. Mater.* **2006**, *18*, 5988−5995.
(8) Hanabusa, K.; Matsumoto, M.; Kimura, M.; Kakehi, A.; Shirai, H. Low Molecular Weight Gelators for Organic Fluids: Gelation Using a Family of Cyclo(dipeptide)s. *J. Colloid Interface Sci.* **2000**, *224*, 231−244.
(9) Hirst, A. R.; Smith, D. K. Solvent Effects on Supramolecular Gel-Phase Materials: Two-Component Dendritic Gel. *Langmuir* **2004**, *20*, 10851−10857.
(10) Kamlet, M. J.; Abbound, J. L. M.; Abraham, M. H.; Taf, R. W. Linear Solvation Energy Relationships. 23. A Comprehensive Collection of the Solvatochromic Parameters, π^*, α, and β, and Some Methods for Simplifying the Generalized Solvatochromic Equation. *J. Org. Chem.* **1983**, *48*, 2877−2887.
(11) Edwards, W.; Lagadec, C. A.; Smith, D. K. Solvent-Gelator Interactions - Using Empirical Solvent Parameters to Better Understand the Self-Assembly of Gel-Phase Materials. *Soft Matter* **2011**, *7*, 110−117.
(12) Yan, N.; Xu, Z.; Diehn, K. K.; Raghavan, S. R.; Fang, Y.; Weiss, R. G. Pyrenyl-Linker-Glucono Gelators. Correlations of Gel Properties with Gelator Structures and Characterization of Solvent Effects. *Langmuir* **2013**, *29*, 793−805.
(13) Hardy, J. G.; Hirst, A. R.; Smith, D. K. Exploring Molecular Recognition Pathways in One- and Two-Component Gels Formed by Dendritic Lysine-Based Gelators. *Soft Matter* **2012**, *8*, 3399−3406.
(14) Bielejewski, M.; Łapiński, A.; Luboradzki, R.; Tritt-Goc, J. Solvent Effect on 1,2-*O*-(1-Ethylpropylidene)-α-D-glucofuranose Organogel Properties. *Langmuir* **2009**, *25*, 8274−8279.
(15) Bielejewski, M.; Tritt-Goc, J. Evidence of Solvent−Gelator Interaction in Sugar-Based Organogel Studied by Field-Cycling NMR Relaxometry. *Langmuir* **2010**, *26*, 17459−17464.
(16) Tritt-Goc, J.; Bielejewski, M.; Luboradzki, R. Interaction of Chlorobenzene with Gelator in Methyl-4,6-*O*-(*p*-nitrobenzylidene)-α-D-glucopyranoside Gel Probed by Proton Fast Field Cycling NMR Relaxometry. *Tetrahedron* **2011**, *67*, 8170−8176.
(17) Bielejewski, M.; Kowalczuk, J.; Kaszyńska, J.; Łapiński, A.; Luboradzki, R.; Demchuk, O.; Tritt-Goc, J. Novel Supramolecular Organogels Based on a Hydrazide Derivative: Non-Polar Solvent-Assisted Self-Assembly, Selective Gelation Properties, Nanostructure, Solvent Dynamics. *Soft Matter* **2013**, *9*, 7501−7514.
(18) Kaszyńska, J.; Łapiński, A.; Bielejewski, M.; Luboradzki, R.; Tritt-Goc, J. On the Relation Between the Solvent Parameters and the Physical Properties of Methyl-4,6-*O*-benzylidene-α-D-glucopyranoside Organogels. *Tetrahedron* **2012**, *68*, 3803−3810.
(19) Tritt-Goc, J.; Kowalczuk, J. Diffusive Diffraction Phenomenon Observed by PGSE NMR Technique in a Sugar-Based Low-Molecular-Mass Gel. *Langmuir* **2012**, *28*, 14039−14044.
(20) Kowalczuk, J.; Jarosz, S.; Tritt-Goc, J. Characterization of Low Molecular-Weight Gelator Methyl-4,6-*O*-(*p*-nitrobenzylidene)-α-D-glucopyranoside Hydrogels and Water Diffusion in Their Networks. *Tetrahedron* **2009**, *65*, 9801−9806.
(21) Steiner, E.; Bouguet-Bonnet, S.; Robert, A.; Canet, D. Relaxometry" Experiments and Analysis of Dispersion Curves: An Illustrative Example of Toluene in Liquid and in Organogel Phases. *Concepts Magn. Reson., Part A* **2012**, *40*, 80−89.
(22) Yemloul, M.; Steiner, E.; Robert, A.; Bouguet-Bonnet, S.; Allix, F.; Jamart-Gregoire, B.; Canet, D. Solvent Dynamical Behavior in an Organogel Phase as Studied by NMR Relaxation and Diffusion Experiments. *J. Phys. Chem. B* **2011**, *115*, 2511−2517.
(23) Terech, P.; Weiss, R. G. Low Molecular Mass Gelators of Organic Liquids and the Properties of Their Gels. *Chem. Rev.* **1997**, *97*, 3133−3159.
(24) Esch, J. H.; Feringa, B. L. New Functional Materials Based on Self-Assembling Organogels: From Serendipity Towards Design. *Angew. Chem., Int. Ed.* **2000**, *39*, 2263−2266.
(25) Kimmich, R.; Anoardo, E. Field-Cycling NMR Relaxometry. *Prog. Nucl. Magn. Reson. Spectrosc.* **2004**, *44*, 257−320.
(26) Maślińska-Solich, J. Condensation and Polycondensation of Terephthaldehyde with Methyl D-Hexopyranosides. *Macromol. Biosci.* **2001**, *1*, 312−321.
(27) Lipkowitz, K. B., Larter, R., Cundari, T. R., Eds. *Reviews in Computational Chemistry*, Vol. *20*; John Wiley & Sons, Inc.: USA, 2004.
(28) Kohanoff, J. *Electronic Structure Calculations for Solids and Molecules. Theory and Computational Methods*; Cambridge University Press: Cambridge, U.K., 2006.
(29) Burke, K.; Werschnik, J.; Gross, E. K. U. Time-Dependent Density Functional Theory: Past, Present, and Future. *J. Chem. Phys.* **2005**, *123*, 062206-1−062206-9.
(30) Runge, E.; Gross, E. K. U. Density-Functional Theory for Time-Dependent Systems. *Phys. Rev. Lett.* **1984**, *52*, 997−1000.
(31) Frisch, M. J.; Trucks, G. W.; Schlegel, H. B.; Scuseria, G. E.; Robb, M. A.; Cheeseman, J. R.; Montgomery, J. A., Jr.; Vreven, T.; Kudin, K. N.; Burant, J. C.; et al. *Gaussian 03*, revision B.03; Gaussian, Inc.: Pittsburgh, PA, 2003.
(32) Becke, A. D. Density-Functional Exchange-Energy Approximation with Correct Asymptotic Behavior. *Phys. Rev. A* **1988**, *38*, 3098−3100.
(33) Becke, A. D. Density-Functional Thermochemistry. III. The Role of Exact Exchange. *J. Chem. Phys.* **1993**, *98*, 5648−5652.
(34) Lee, C.; Yang, W.; Parr, R. G. Development of the Colle-Salvetti Correlation-Energy Formula Into a Functional of the Electron Density. *Phys. Rev. B* **1988**, *37*, 785−789.
(35) Scott, A. P.; Radom, L. Harmonic Vibrational Frequencies: An Evaluation of Hartree Fock, Møller-Plesset, Quadratic Configuration Interaction, Density Functional Theory and Semiempirical Scale Factors. *J. Phys. Chem.* **1996**, *100*, 16502−16513.
(36) Sun, R.; Yao, J.; Li, S.; Gu, R. Raman Spectroscopic and Density Functional Theory Studies on a Benzothiazole-2-thione Derivative. *Vib. Spectrosc.* **2008**, *47*, 38−43.
(37) Michalska, D.; Wysokinski, R. The Prediction of Raman Spectra of Platinum (II) Anticancer Drugs by Density Functional Theory. *Chem. Phys. Lett.* **2005**, *403*, 211−217.
(38) Polavarapu, P. L. Ab Initio Vibrational Raman and Raman Optical Activity Spectra. *J. Phys. Chem.* **1990**, *94*, 8106−8112.
(39) Stejskal, E. O.; Tanner, J. E. Spin Diffusion Measurements: Spin Echoes in the Presence of a Time-Dependent Field Gradient. *J. Chem. Phys.* **1965**, *42*, 288−292.
(40) Wende, C.; Schonhoff, M. Dynamics of Water in Polyelectrolyte Multilayers: Restricted Diffusion and Cross-Relaxation. *Langmuir* **2010**, *26*, 8352−8357.
(41) Bennett, K. M.; Schmainda, K. M.; Bennett, R.; Rowe, D. B.; Lu, H. B.; Hyde, J. S. Characterization of Continuously Distributed Cortical Water Diffusion Rates with a Stretched-Exponential Model. *Magn. Reson. Med.* **2003**, *50*, 727−734.
(42) Nyden, M.; Soderman, O. An NMR Self-Diffusion Investigation of Aggregation Phenomena in Solutions of Ethyl(hydroxyethyl)-cellulose. *Macromolecules* **1998**, *31*, 4990−5002.
(43) Omari, R. A.; Aneese, A. M.; Grabowski, C. A.; Mukhopadhyay, A. Diffusion of Nanoparticles in Semidilute and Entangled Polymer Solutions. *J. Phys. Chem. B* **2009**, *113*, 8449−8452.
(44) Noack, F. NMR Field-Cycling Spectroscopy: Principles and Applications. *Prog. NMR Spectrosc.* **1986**, *18*, 171−276.
(45) Anoardo, E.; Galli, G.; Ferrante, G. Fast-Field-Cycling NMR: Applications and Instrumentation. *Appl. Magn. Reson.* **2001**, *20*, 365−404.
(46) Tavernier, H. L.; Fayer, M. D. Solute-Solute Spatial Distribution in Hydrogen Bonding Liquids Probed with Time-Dependent

Intermolecular Electron Transfer. *J. Chem. Phys.* **2000**, *114*, 4552−4564.
(47) Padró, J. A.; Saiz, L.; Guàrdia, E. Hydrogen Bonding in Liquid Alcohols: a Computer Study. *J. Mol. Struct.* **1997**, *416*, 243−248.
(48) Usacheva, T. M.; Lifanova, N. V.; Zhuravlev, V. I.; Matveev, V. K. A Dielectric Study of the Structure of Propylene Glycol. *Russ. J. Phys. Chem. A* **2010**, 1194−1201.
(49) Li, X. Q.; Zhang, X.; Ghosh, S.; Wurthner, R. Highly Fluorescent Lyotropic Mesophases and Organogels Based on J-Aggregates of Core-Twisted Perylene Bisimide Dyes. *Chem.—Eur. J.* **2008**, *14*, 8074−8078.
(50) Babu, S. S.; Kartha, K. K.; Ajayaghosh, A. A. Excited State Processes in Linear π-System-Based Organogels. *J. Phys. Chem. Lett.* **2010**, *1*, 3413−3424.
(51) Kobayashi, H.; Friggeri, A.; Koumoto, K.; Amaike, A.; Shinkai, S.; Reinhoudt, D. N. Molecular Design of "Super" Hydrogelators: Understanding the Gelation Process of Aobenzene-Based Sugar Derivatives in Water. *Org. Lett.* **2002**, *9*, 1432−1426.
(52) Kamiguchi, K.; Kuroki, S.; Satoh, M.; Ando, I. Structural Characterization of Inhomogeneous Poly(methyl methacrylate) Gels by Time-Dependent Diffusion NMR Spectroscopy. *Macromolecules* **2009**, *42*, 231−235.
(53) Mitra, P. P.; Sen, P. N.; Schwartz, L. M.; Ledoussal, P. Diffusion Propagator as a Probe of the Structure of Porous Media. *Phys. Rev. Lett.* **1992**, *68*, 3555−3558.
(54) Abragam, A. *The Principles of Nuclear Magnetism*; Oxford University Press: Oxford, U.K., 1996.
(55) Kruk, D.; Meier, R.; Rossler, E. A. Translational and Rotational Diffusion of Glycerol by Means of Field Cycling ^{1}H NMR Relaxometry. *J. Phys. Chem. B* **2011**, *115*, 951−957.
(56) D'Agostino, C.; Mitchell, J.; Gladden, L. G.; Mantle, M. D. Hydrogen Bonding of Porous Coordination Polymer Crystals by Coordination Modulation. *J. Phys. Chem. C* **2012**, *116*, 8975−8982.